Multiobjective Path Optimization for Critical Infrastructure Links with Consideration to Seismic Resilience

Wang, Zengfu; Wang, Qing; Zukerman, Moshe; Guo, Jun; Wang, Yu; Wang, Gang; Yang, Jun; Moran, Bill

Multi-Objective Path Optimization for Critical Infrastructure Links with Seismic Resilience

Zengfu Wang

School of Automation, Northwestern Polytechnical University, Xi'an, China

Qing Wang, Moshe Zukerman

Department of Electronic Engineering, City University of Hong Kong, Hong Kong, China

Jun Guo

College of Computer Science and Technology, Dongguan University of Technology, Dongguan, China

Yu Wang*

Department of Architecture and Civil Engineering, City University of Hong Kong, Hong Kong, China

Gang Wang

Department of Civil and Environmental Engineering, Hong Kong University of Science and Technology, Hong Kong, China

Jun Yang

Department of Civil Engineering, The University of Hong Kong, Hong Kong, China

&

Bill Moran

School of Engineering, RMIT University, Australia

Abstract—**With an ever-increasing level of globalization in almost every aspect of the economy, long-haul trans-regional, -national, or -continental links have become an essential part of modern infrastructures. Such critical links, if broken, can have grave social and economic consequences. In this paper, we study the generic problem of path optimization for a critical infrastructure link between two locations on the surface of the Earth that crosses an earthquake-prone area. The problem has two (conflicting) objective functions, one for minimizing the construction cost of the link and the other for minimizing the number of potential repairs along the link in the wake of earthquakes. The model uses ground motion intensity measures for estimating the link repair rate, and triangulated manifolds for representing the surface of the Earth. We approach the multi-objective variational problem by first converting it into a single objective variational problem using the weighted sum method. Then, we show that the problem can be further transformed into an Eikonal equation and solved by a computationally efficient algorithm based on the fast marching method. Extensive simulations are performed on real-world three-dimensional geographical data, from which we obtain Pareto optimal solutions that provide insight and guidance to design tradeoffs between cost effectiveness and seismic resilience.**

Index Terms—**Critical infrastructure links, path optimization, multi-objective optimization, cost effectiveness, seismic resilience.**

I. Introduction

Critical infrastructures such as electricity, oil, gas, telecommunications, transportation and water are essential to the functioning of modern economies and societies. As the world is increasingly interconnected, long-haul trans-regional, -national, or -continental links are playing a crucial role in transporting critical resources and information from one location to another. For example, it is known that submarine telecommunications cables carry over 95% of the global voice and data traffic (Carter et al., 2009). Russian gas that is delivered through the trans-European pipeline accounts for over a quarter of the total European consumption (Cobanli, 2014). Such critical infrastructure links are vulnerable to disasters (Neumayer et al., 2011) and, if broken, can have severe social and economic consequences.

Among various natural disasters, earthquakes often cause the most catastrophic effects. For example, in 1987, the Ecuador earthquake resulted in the damage of nearly 70 km of the Trans-Ecuadorian oil pipeline. Loss of the pipeline deprived Ecuador of 60% of its export revenue, and it took five months to reconstruct the pipeline (Schuster, 1991). In 2006, the Hengchun/Taiwan earthquake damaged eight submarine cables with a total of 18 cuts. As a result, Internet services in Asia were severely disrupted for several weeks, affecting many Asian countries (Qiu, 2011). It was estimated that, for a well-developed economy that is largely reliant on the Internet, one week of Internet blackout can cause losses of over 1% of annual GDP (mi2g, 2005; Dübendorfer, 2005). These events

*To whom correspondence should be addressed. E-mail: yuwang@cityu.edu.hk

signify the impacts of earthquake hazards and the importance of enhancing the seismic resilience of critical infrastructure links (Cao et al., 2013; Cao, 2015; Cao et al., 2016).

In this paper, we study the generic problem of path optimization for a critical infrastructure link between two locations on the surface of the Earth that crosses an earthquake-prone area. The focus is on the set of infrastructure links, such as undersea cables and long-haul oil/gas/water pipelines, where surface distance is a reasonable measure of the length of a link. For such a practically important problem, we are not aware of any theoretically sound approach proposed in the literature that takes into consideration both cost effectiveness and seismic resilience. To address this gap, we formulate the problem as a multiobjective variational problem where we aim to find the set of Pareto optimal paths for the infrastructure link with two objective functions.

- The first objective is to minimize the cost associated with the construction of the infrastructure link. Connecting the two locations by a geodesic, i.e., the route with the shortest surface distance, may minimize the construction cost but can increase the risk of damage or break in the event of an earthquake.
- The second objective is to minimize the number of potential failures (hence repairs) along the infrastructure link in the wake of earthquakes, which may serve as an index of the cost associated with the loss and reconstruction of the link in the event of failures.

In general, the larger the number of failures, the larger is the mean time to restore the link (LaPerrière, 2007). Thus, the second objective in our context is related to the notion of seismic resilience (Bruneau et al., 2003), which implies the ability of the link to return to normal condition after an earthquake shock that disrupts its operation.

Our model is built on the state of the art in geographic information systems (GIS) for terrain approximation (Chang, 2013) and the latest developments in earthquake engineering for seismic hazard assessment (Villaverde, 2009). Specifically, the model considers triangulated manifolds for representing the surface of the Earth and ground motion intensity measures for estimating the link repair rate in the event of an earthquake. Based on this model, we approach the multi-objective variational problem by first converting it into a single objective variational problem using the weighted sum method (Miettinen, 1999). Then, we show that the problem can be further transformed into an Eikonal equation and solved by a computationally efficient algorithm based on the well-established fast marching method (Kimmel and Sethian, 1998; Sethian, 1999a). This enables us to obtain Pareto optimal solutions that provide flexibility in path optimization for a critical infrastructure link, taking into consideration the fundamental tradeoff between cost effectiveness and seismic resilience.

The rest of the paper is organized as follows. In Section II, we discuss the related work. In Section III, we present and motivate the problem of laying a link between two nodes, and the multi-objective optimization approach we use in this paper. In Section IV, we describe the model. In Section V, we provide details of the problem formulation and solution. Simulation results are presented in Section VI. Finally, we draw conclusions in Section VII.

II. Related Work

Much work has been done on understanding the damage of infrastructure links by past earthquakes. The work of Liu (2009) summarized main factors that impact submarine cables based on their performance in three past earthquakes, including the 2006 Hengchun earthquake, the 2004 Sumatra earthquake and the 1929 Grand Banks earthquake. The work of Chen et al. (2002) investigated the damage patterns of natural gas and water pipelines in the 1999 Chi-Chi earthquake, and conducted statistical analysis to understand the correlation between repair rates and seismic parameters. The work of Carter et al. (2014) investigated the effect of damaging submarine flows on submarine cables in the 2006 Pingtung earthquake, and presented insights regarding the causes, frequency, and behavior of submarine flows. The work of Kobayashi (2014) reported the experience of infrastructure damage caused by the 2011 Tohoku earthquake. Hwang et al. (2004) investigated damage to natural gas pipelines due to ground shaking effects, and performed regression analyses of pipe repair rates to derive seismic vulnerability functions based on pipe repair data and recorded strong motion data in the 1999 Chi-Chi earthquake.

Through modeling and analyzing the vulnerability, researchers have also worked on evaluation of potential damage to current infrastructure links by earthquakes. Lanzano et al. (2013) analyzed the interaction of earthquakes with natural gas pipelines in terms of the likelihood of the loss of containment with respect to peak ground velocity. Esposito et al. (2015) analyzed the vulnerability of gas networks via fragility curves and evaluated their seismic performance via computer-aided simulation. Wang and O'Rourke (2008); Wang and Au (2009) proposed methods to identify critical links of water supply with a relatively large damage probability under an earthquake. Adachi and Ellingwood (2009) provided an evaluation of the serviceability of the municipal water distribution system in Shelby County, Tennessee considering spatial correlation in seismic intensity and demand. A case study for a town in suburb of Algiers has been presented in Zohra et al. (2012) for a proposed method based on the identification of parameters to assess the seismic vulnerability of water pipeline network. Cavalieri et al. (2014) presented a comparison of five seismic performance assessment models for power networks.

The work mentioned above focused on modeling, analysis or evaluation of potential damages and vulnerability for a given infrastructure link system, but not on path optimization for a critical infrastructure link which is the problem considered in this paper. Although the former can provide insights and support for the latter, however, they are much more distinct in methodologies.

A closely related problem in civil and infrastructure engineering is pipeline route selection. State-of-the-art approaches are in general computer-assisted heuristics utilizing GIS technology (Macharia, 2014; Balogun et al., 2012; Yildirim et al., 2007; Dey and Ogunlana, 1999). Specifically, they are based on weighting factors considered to be affecting the route and then applying raster-based path analysis to find the least accumulative cost path using the Dijkstra's shortest path algorithm (Chang, 2013). However, the effects of earthquakes were considered by these publications. A similar approach was used by Zhao et al. (2016) for cable route selection considering cost minimization and earthquake survivability. A major limitation of the raster-based path analysis is that a path is restricted to use either a lateral link or a diagonal link when moving from one cell to its adjacent cells. Our approach in this paper suits a broader class of critical infrastructure links including undersea cables and uses a theoretically sound methodology with guaranteed optimality. In Cao et al. (2013); Cao (2015); Cao et al. (2016), not raster-based resilient path design for cables are proposed but it is assumed that the topology lies on a two-dimensional plane. We address the problem of provisioning links based on a more accurate model that represents the surface of the Earth as a two-dimensional manifold in three-dimensional space.

III. THE MULTI-OBJECTIVE OPTIMIZATION APPROACH

As discussed in the Introduction, the optimization of the path of a link between two nodes in an earthquake prone region is based on multiple objectives. In particular, we consider the following two objective functions. The first is the laying cost (applicable to e.g. a telecommunication cable), or construction cost (for e.g. an oil pipeline). For brevity, thereafter, we will use the term *laying cost* to refer to both laying and construction cost. The second objective function is an index associated with the estimation of future number of repairs (or failures) of the link in a given time period (e.g. 100 years). While the first objective is about cost incurred during laying, the second objective is about cost incurred in the (potentially, long term) future.

A. Why multi-objective optimization?

There are various factors associated with estimation of the first objective, namely, the laying cost. The length of the link is clearly a factor here, but it is not the only factor as the laying cost can vary from one location to another based on ground/soil condition, requirement for security arrangements, licensing and various other factors. The reason that we need to address the problem as a multi-objective optimization is the second objective function.

While the dollar value of the first objective is relatively clear, it is not so simple to assign a dollar value to potential link failures, mainly because different stakeholders have significantly different views of the cost of link failures. While for a telecom cable owner, cable breaks incur cost associated with the repair needed minus any insurance payment received, for an insurance company the cost consequence may be higher, and for the society, government or public the cost of cable failures can be much higher, as one week of Internet shutdown has been estimated at 1.2% of annual GDP (mi2g, 2005; Dübendorfer, 2005), which means billions of dollars. In addition, failure of infrastructure links can lead to loss of lives in various cases of natural disasters. Given the multiplicity of stakeholders with different exchange rates between link failure risks and dollar values, it is appropriate to use a methodology based on multi-objective optimization that leads to a set of Pareto optimal solutions. Such optimal solutions provide for a given budget for laying cost, the planned path that minimizes the risk (as measured by predicted number of repairs), and for each given predicted number of repairs, the planned path that minimizes the laying cost.

B. The second objective

While the choice of the first objective is relatively straightforward the choice of the second objective of the predicted number of repairs requires some discussion. Larger predicted number of repairs (failures) indicates both potential costs of repairs, as well as link downtime that may have significant societal cost. As an illustration, after the 2006 Taiwan Earthquake, eight submarine cable systems were found to be damaged with a total of 18 cable cuts (Qiu, 2011). The repair for each cable cut was expected to require around seven days (LaPerrière, 2007). Although some repair can be done in parallel, it still took over a month to achieve full restoration of connectivity following the Taiwan earthquake.

Accordingly, we adopt the view that a reasonable index to represent the level of damage caused by an earthquake is the total number of repairs (or failures) of the link. To estimate the number of repairs, we rely on data of ground motion in the past during a certain period of time, or simulations based on given geological knowledge. We are, in fact, using past data to predict events in the future. Nevertheless, this is considered reasonable, as the geology does not change significantly over time.

Since the relevant period of time the ground motion data has been measured (or simulated) applies to all points in the map equally, and since the data is based on the past, we henceforth use the abbreviated term of *total number of repairs* without mentioning the period of time and the fact that it is "potential". This is our second objective to be optimized.

To calculate total number of repairs for a link, we will use the term *repair rate* (Wang and O'Rourke, 2008; Fragiadakis and Christodoulou, 2014; Jeon and O'Rourke, 2005; Esposito, 2011; Cimellaro et al., 2014) to indicate the predicted number of repairs per unit length of the link over a fixed time period into the future. An alternative term, less used in the earthquake literature is *failure rate*. In addition, for a specific link, the repair rate varies for different points on the link and depends on various factors as well, such as the geology, link material and ground/soil conditions. In another

context considering earthquakes effects, the repair rate has been widely used to assess reliability of water supply networks (Wang and O'Rourke, 2008; Fragiadakis and Christodoulou, 2014; Jeon and O'Rourke, 2005), and to analyze the risk to gas distribution networks (Esposito, 2011; Cimellaro et al., 2014).

To estimate the repair rate which we use for estimating the total number of repairs of a link, we rely on data of ground motion in the past during a certain period of time, or simulations based on given geological knowledge. As in Section IV, we also take advantage of the extensive work of the United States Geological Survey (USGS) analysts that develop models for the potential effects of future earthquakes.

IV. Modeling

In this section, we describe the models we introduce for the landforms, laying cost, and the potential required repairs.

A. Landform model

We approximate the region of the Earth's surface (including the sea bed) under consideration as a closed, connected (Greenspan, 2000), two-dimensional manifold $\mathbb{M}$ in three-dimensional Euclidean space $\mathbb{R}^3$, uniquely represented by a continuous, single-valued function $z = \xi(x, y)$, where z is the elevation and x and y are the Cartesian coordinates (Florinsky, 2012). In particular, caves, grottos, tunnels etc. are ignored.

As information about the landforms is always available in a quantized form (discrete grid), we use a *triangulated piecewise-linear two-dimensional manifold* to approximate the Earth's landforms. Such triangulated manifold models are widely used to represent topography and terrain in GIS and other related fields, as they makes it easier than other available models (e.g. the regular grid model) to consider rough surfaces and to accommodate irregularly spaced elevation data (Peucker et al., 1978; Lee, 1991). We further assume that the triangulated manifold model is *complete*; that is, it is a connected triangulated manifold surface $\mathbb{M}$ in $\mathbb{R}^3$ that consists of faces, edges and vertices and satisfies the following conditions (Martínez et al., 2005).

- There are no isolated vertices.
- Each edge belongs to exactly one triangle or is shared by just two triangles. Any two triangles intersect in a common vertex or edge, or not at all.
- Any two points on the surface, are connected by a path (possible through the middle of a triangle) on the surface connecting the two points.

These conditions do not pose significant modeling limitations because areas that do not satisfy these conditions, such as cliff faces, will be avoided by the link in any case. The particular details of how to address such areas in the model will be discussed below.

B. Laying cost model

As mentioned above, the laying cost is affected by various factors and varies from one location to another. For $(x, y, z) \in \mathbb{M}$, we define a function $h(x, y, z)$ to represent the link cost at point (x, y, z), where $z = \xi(x, y)$. This function gives the path planner the flexibility to consider different laying cost for different locations. For example, there are many areas that links (submarine telecommunications cables) must avoid, or require high costs (Yung, 2011). They include:

- areas that are of high ecological value (e.g. coral communities)
- areas where special and costly licenses are required
- areas with wind or underwater turbines
- marine vessel fairways
- incompatible seabed (e.g. rocky areas)
- marine borrow area (e.g. gazetted dredging and sediment disposal area and sand deposit area)
- anchorage areas and fishery areas.

Setting appropriately high values to the function $h(x, y, z), z = \xi(x, y)$ will enable avoidance of such areas, or at least imposition of a high cost. In areas where the cost of the link is only its length, we set $h(x, y, z)$ equal to a constant value, e.g., $h(x, y, z) = 1$, where $z = \xi(x, y)$.

Let node A and node B be two fixed points with coordinates X_A and X_B in $\mathbb{M}$, that have to be connected by a link, defined as a (Lipschitz continuous (Eriksson et al., 2013)) curve γ in $\mathbb{M}$ that connects the points A and B. Let $\mathbb{H}(\gamma)$ be the laying cost of the link γ. We assume:

- The laying cost $\mathbb{H}(\gamma)$ of the link γ is quantified in terms of the cost per unit length at every point on the link, and is location dependent.
- For any particular point on the link, S, the laying cost per (arbitrarily) small length ds, $d\mathbb{H}(\gamma)$, is calculated as the product of the laying cost $h(X_S)$ and length ds, i.e., $h(X_S)ds$. Here we use capital letters (e.g. S, X, X_S,A, and B) to denote points, but we use small letters (e.g., x, y, z) to denote the actual coordinates.

Then the laying cost of the link γ is the integral of the laying cost at each point along the path of the link. That is,

$$\mathbb{H}(\gamma) = \int_\gamma h(X)ds, \tag{1}$$

where $h(X) \in \mathbb{R}^1_+$ is the laying cost at location X.

C. Link repair model

Now we discuss the correlation of ground movements resulting from earthquakes with the repair rate.

Since the link is laid on the surface of the Earth, the repair rate $g(X)$ is defined on the surface introduced previously, and therefore as a function of the coordinates x and y: $g(X) = g(x, y, z), z = \xi(x, y)$. Typically, after an earthquake event, the area affected can be subdivided into many cells,

and in each cell, repair rate of a link in the cell is determined by dividing the number of repairs by the length of the link in the cell. Repair rate is to a reasonable first approximation a function of link material, ground/soil conditions, diameter, and ground movement, as quantified by Peak Ground Velocity (PGV) and Permanent Ground Deformation (PGD) (Alliance, 2001).

Some publicly available information on the repair rate and its correlation with ground movement can be found in the context of water and gas pipelines (Wang and O'Rourke, 2008; Fragiadakis and Christodoulou, 2014; Jeon and O'Rourke, 2005). Many ground motion parameters have been used for relating repair rate with seismic intensity (Pineda-Porras and Najafi, 2010). In this paper, PGV is adopted to derive the repair rate since a significant correlation has been found between the two (O'Rourke et al., 1998; Toprak, 1998; Toprak and Taskin, 2007) and PGV is widely used for deriving repair rate in the literature (Alliance, 2001; Jeon and O'Rourke, 2005; Pineda-Porras and Najafi, 2010). For example, American Lifelines Alliance (Alliance, 2001) proposes the following linear equation:

$$g(X) = \frac{0.00187}{0.3048} \cdot k \cdot \left(\frac{v(X)}{2.54}\right) \qquad (2)$$

where $g(X)$ is the repair rate at location X, and is normalized to the number of repairs per km; $v(X)$ (cm/s) is the PGV at location X; k is a coefficient based on the pipe material, joint type, soil type and conditions and diameter size, determined experimentally. The recommended model parameters can be found in (Alliance, 2001). An example of PGV map of United States, derived based on Peak Ground Acceleration (PGA) (http://www.usgs.gov/) data provided by USGS, is shown in Fig. 1. For specific details on how we convert data from PGA to PGV see Section VI below. In Fig. 1, different colors represent different levels of PGV. We can read the value of PGV (in cm/s) for a site from the color bar on the right of Fig. 1. The gradual change of the color of the color bar, which is from blue to red, corresponds to increases of the PGV from the minimum value to the maximum value.
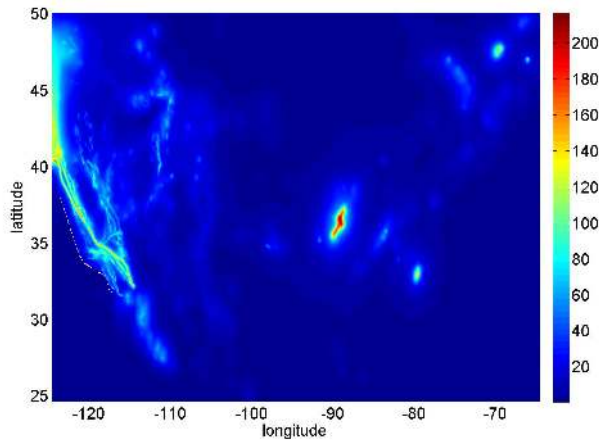

Fig. 1. The shaded surface map of PGV of United States (cm/s). Data is provided by USGS.

Note that the application of our method is not limited to PGV and other information on ground motion can be used to estimate the repair rate. It is apparent that the more accurate the estimation of repair rate is, the more reliable are the path planning results.

Let $\mathbb{G}(\gamma)$ be the total number of repairs of the link γ. The assumptions we made previously for the laying cost of the link $\mathbb{H}(\gamma)$, apply also for the total number of repairs; namely, we assume,

- The total number of repairs $\mathbb{G}(\gamma)$ of the link γ is quantified in terms of the repair rate at every point on the link, and is location dependent.
- For any particular point on the link, S, the number of repairs per (arbitrarily) small length ds, $d\mathbb{G}(\gamma)$, is calculated as the product of the repair rate $g(X_S)$ and length ds, i.e., $g(X_S)ds$.

Then the total number of repairs of the link γ is the integral of the repair rate at each point along the path of the link. That is,

$$\mathbb{G}(\gamma) = \int_{\gamma} g(X)ds, \qquad (3)$$

where $g(X) \in \mathbb{R}^1_+$ is the repair rate at location X.

We also note that the larger the total number of repairs, the smaller the link survival probability defined as one minus the probability of the event of at least one repair (Røstum, 2000; Fragiadakis and Christodoulou, 2014).

V. PROBLEM FORMULATION AND SOLUTION

Based on the models of landforms, laying cost, and the potential required repairs, our multi-objective optimization problem of minimizing the laying cost and the total number of repairs is as follows,

$$\text{(Problem 1)} \qquad \min_{\gamma} \Phi(\gamma) = \big(\mathbb{H}(\gamma),\ \mathbb{G}(\gamma)\big),$$
$$\text{s.t. } \gamma(A) = X_A, \gamma(B) = X_B.$$

To calculate the laying cost and the total number of repairs of the link γ, we parametrize the curve γ as functions of arc length, s; that is, every point $X \in \gamma$ can be represented by arc length s as $X = X(s)$. Such a parametrization is also known as the *natural definition* of a curve (Burago et al., 2001). Then the laying cost and total number of repairs of the link γ are rewritten as,

$$\mathbb{H}(\gamma) = \int_0^{l(\gamma)} h(X(s))ds,\ \mathbb{G}(\gamma) = \int_0^{l(\gamma)} g(X(s))ds, \quad (4)$$

where $h(X(s)), g(X(s)) \in \mathbb{R}^1_+$ are the laying cost and the repair rate at location $X(s)$, respectively, and $l(\gamma)$ is the length of the link γ.

This problem can be formulated as a multi-objective variational optimization problem for which calculus of variations approaches are applicable. In the following, we describe the

methodology we use for path planning that solves Problem 1.

Since Problem 1 has multiple objectives, in general it is impossible to simultaneously optimize both the laying cost and the total number of repairs. Therefore, Pareto optimal solutions are sought. A standard method to solve Problem 1 is to formulate it as a single-objective function optimization problem through the weighted sum method, i.e.,

(Problem 2) $\quad \min_{\gamma} \Phi(\gamma) = \int_0^{l(\gamma)} f(X(s))ds,$

$$\text{s.t. } X(0) = X_A, X(l(\gamma)) = X_B,$$

where $f(X(s)) = c \cdot h(X(s)) + g(X(s))$ and $c \in \mathbb{R}_+^1$. By the theory of multi-objective variational optimization (Bector and Husain, 1992), if γ^* is an optimal solution for Problem 2, then it is Pareto optimal for the laying cost $\mathbb{H}$ and the total number of repairs $\mathbb{G}$. With different weights c in Problem 2, distinct Pareto optimal solutions are produced.

In consequence of the formulation of Problem 2 as a single objective variational problem, the solution paths that minimize the integral are the minimum cost paths. We emphasize here that Problem 2 is a continuous problem. The fast marching method (FMM), a consistent and computational efficient numerical algorithm proposed by Sethian (Sethian, 1999b, 1996; Kimmel and Sethian, 1998; Sethian, 1999a), for solving the Eikonal equation, is adopted here to solve Problem 2 in a continuous space. On the one hand, FMM can be proved to converge to the continuous physical (viscosity) solution as the grid step size tends to zero. On the other hand, FMM has optimal computational complexity, which is $O(N \log N)$, where N is the total number of discretized grid points of $\mathbb{M}$ (Sethian, 1999b).

A. Derivation of the Eikonal equation

The first step in applying FMM is to transform the variational Problem 2 to a partial differential equation called the Eikonal equation. For any point $S \in \mathbb{M}$, a cost function $\phi(S)$ that represents the minimal cumulative cost to travel from one end point B of the link to point S is defined as,

$$\phi(S) = \min_{\beta} \int_0^{l(\beta)} f(X(s))ds, \qquad (5)$$

where $\beta \in \text{Lip}([0, +\infty); \mathbb{M})$ is a Lipschitz continuous path parameterized by its length, $\|\beta'(s)\| = \|\frac{d\beta(s)}{ds}\| = 1$, $X(0) = X_B$, and $X(l(\beta)) = X_S$. By Equation (5) and the definition of f, and applying the fundamental theorem of the Calculus of Variations, Kimmel and Sethian (2001) have shown that $\phi(S)$ is the viscosity solution of the following Eikonal equation,

$$\|\nabla\phi(S)\| = f(S) = c \cdot h(S) + g(S), \ \phi(B) = 0, \quad (6)$$

where ∇ is the gradient operator and $\| \cdot \|$ is the 2-norm. For any point S, $\phi(S)$ is called the *level set function*; that is, $\{S \in \mathbb{M} : \phi(S) = a\}$ is a curve composed of all the points that can be reached from point B with minimal cost equal

to a. The optimal path(s) is (are) along the gradient of $\phi(S)$; i.e., orthogonal to the level curves. More precisely, we can construct the optimal path(s) by tracking backwards from S to B, solving the following ordinary differential equation

$$\frac{dX(s)}{ds} = -\nabla\phi, \quad \text{given } X(0) = X_S \qquad (7)$$

until point S, is reached, where $X \in \mathbb{M}$. The optimal path(s) from A to B for Problem 2 is (are) then obtained by letting $S = A$.

B. The update scheme

The partial differential Eikonal equation cannot be solved analytically for an arbitrary non-negative cost function f. In fact, its solution does not necessarily need to be differentiable. Therefore, we adopt a numerical method to solve the Eikonal equation.

In Section IV, we have approximated landforms by a complete two dimensional triangulated manifolds, deriving a discretized grid model of the region $\mathbb{M}$. Accordingly, an update scheme to calculate the value of ϕ at each grid point is required. In Kimmel and Sethian (1998), to compute a geodesic path on triangulated manifolds, Sethian proposes a monotone update procedure on a triangulated mesh to approximate the gradient in (6), from which the viscosity solution is obtained. The resulting path converges to the exact shortest path as the triangulation is refined. Here, we apply it to equation (6) of Problem 2.

For acute triangles of the triangulated landform manifolds, the update procedure is as follows. We aim first to update the value of $\bar{\phi}$ of a center vertex, such as vertex V shown in Fig. 2, which is the intersection point of several triangles. For each of these triangles, for example the triangle $\triangle VV_1V_2$ in Fig. 2, we calculate the solutions of the following quadratic equation.

$$a'\phi^2 + b'\phi + c' = 0, \qquad (8)$$

where

$$a' = (a^2 + b^2 - 2ab\cos\theta),$$
$$b' = 2b(\bar{\phi}(V_2) - \bar{\phi}(V_1))(a\cos\theta - b),$$
$$c' = b^2((\bar{\phi}(V_2) - \bar{\phi}(V_1))^2 - f(V)^2a^2\sin^2\theta).$$

We use this triangle to update the value of $\bar{\phi}$ for vertex V as follows. If $\phi > \bar{\phi}(V_2) - \bar{\phi}(V_1)$ and

$$a\cos\theta < \frac{b(\phi - (\bar{\phi}(V_2) - \bar{\phi}(V_1)))}{t} < \frac{a}{\cos\theta},$$

then

$$\bar{\phi}(V) = \min\{\bar{\phi}(V), \phi + \bar{\phi}(V_1)\}. \qquad (9)$$

Otherwise,

$$\bar{\phi}(V) = \min\{\bar{\phi}(V), bf(V) + \bar{\phi}(V_1), af(V) + \bar{\phi}(V_2)\}. \quad (10)$$

Since each triangle containing the vertex V can produce a possible update value $\bar{\phi}$ for that vertex, in order to meet the

upwind criterion (Sethian, 1999b), the smallest new value $\bar{\phi}$ for V is chosen.
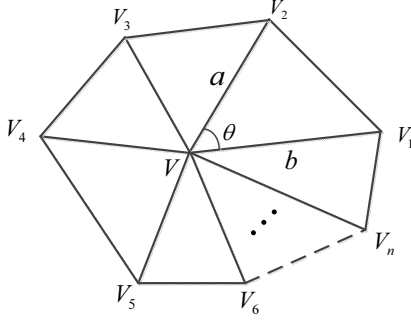

Fig. 2. Illustration of acute triangulation around center vertex on landform manifolds.

For the update procedure described above, an acute triangulation is required, because the values of both vertex V_1 and vertex V_2 are needed to update the value of V simultaneously. Although there is a guarantee for the existence of acute triangulations for a general polyhedral surface (Saraf, 2009), no polynomial algorithm for constructing such triangulations has been found. For a given specific initially triangulated landform manifold with non-acute triangles, we may split every obtuse triangle into acute ones. If not, an "unfolding" step is necessary for the remaining obtuse angles (Kimmel and Sethian, 1998). A refinement for the splitting of obtuse angles is provided in Xin and Wang (2007). Details can be found in Kimmel and Sethian (1998); Sethian (1999a); Xin and Wang (2007).

C. Algorithm for path planning

Given the update scheme described above, and the initial value $\phi(B) = 0$, the next step is to calculate the value of ϕ at each point S on the triangulated grid of $\mathbb{M}$. From the non-negativity of f and the upwind difference structure, it is useful to imagine ϕ as a wave function, and note that the wave propagates "one way"; that is, from B outwards, and the value of ϕ at any point depends only on adjacent vertices having smaller values. Based on these observations, Sethian (1996) proposed to update the values of the grid points in a way similar to the Dijkstra shortest path algorithm, and named it the *Fast Marching Method*. The algorithm is described as follows:

1) Initialization. All boundary points (e.g., B) are tagged as *Frozen*. Their nearest neighbors (one grid point away) are then tagged as *Near* and the value of these nearest neighbors are updated by solving (8) using *Frozen* points. The remaining grid points are tagged as *Far*;
2) The point with minimum value ϕ among all points with the tag *Near* is retagged to *Frozen*. If there are no such points, the algorithm is complete. If there is exactly one such point, return to **Step 3**. If there are more than one such point, pick one arbitrarily and return to **Step 3**;

3) Find the nearest neighbors that are either *Far* or *Near* of the *Frozen* point found in **Step 2**, and update their values by solving equation (8) using the *Frozen* points and change their tag to *Near* if they are *Far*;
4) Go back to **Step 2**.

Based on the above procedure, the status of points can only change from *Far* to *Near* or from *Near* to *Frozen*. The tags of points cannot be changed in an opposite direction, i.e., from *Near* to *Far* or from *Frozen* to *Near*. In **Step 3**, each updated point is assigned a new value that is less than its previous value. If the point is *Far*, it is tagged *Near*. In **Step 2**, the tag of one and only one point is changed in each loop. Therefore, the FMM is a one-pass algorithm; it does not have to "go back and correct an accepted value (of a *Frozen* point)". Since we can locate the grid point with minimum value ϕ among all points with tag *Close* (in **Step 2**) using a heap algorithm with time complexity $O(N)$, it is easily seen that FMM can be implemented with time complexity $O(N \log N)$ if N is the total number of points in the grid (Sethian, 1999a).

Based on the landforms model, the laying cost model and the potential required repairs model given in Section IV and the FMM introduced above, we provide an algorithm, called **Algorithm** 1, for path planning on a topographic surface. As we said at the beginning of this section, by setting different values of c in Problem 2, we can obtain different Pareto optimal solutions of the laying cost and the total number of repairs. However, because of numerical errors when running Algorithm 1, some of the results may be dominated by others. Such results are ignored and only the non-dominated results are presented to obtain the approximate Pareto front which is also called *non-dominated front*. Examples of such non-dominated optimal solutions will be provided in the next section.

We summarize the approach we used to solve the problem of how to lay a critical infrastructure link to connect two points across an earthquake prone area in Fig. 3.

VI. APPLICATIONS

In this section, we illustrate the applications of Algorithm 1 to scenarios based on 2D and 3D landforms. We start with a simple case of 2D topography, where the PGV data is obtained by simulations by the Probabilistic Seismic Hazard Analysis (PSHA) method (Baker, 2008). Then, we apply the algorithm to two scenarios of 3D landforms based on earthquake hazard assessment data from USGS. Without loss of generality, we set the laying cost at each point in the region of interest to be uniform, i.e., $\forall S \in \mathbb{M}, h(S) = 1$. The length and the total number of repairs of different links are estimated. We take advantage of the low complexity of FMM, and generate many runs for different c values to obtain the set of non-dominated optimal solutions.

Algorithm 1 – Algorithm for path planning on surface $\mathbb{M}$.

Input: Region $\mathbb{D}$ (modelled as $\mathbb{M}$), spatially distributed PGV data on $\mathbb{M}$, mesh size Δ_x, Δ_y, start point A, end point B, c, step size τ;

Output: Path γ with minimum cost;

1: Discretize $\mathbb{M}$ rectangularly with Δ_x in x and Δ_y in y, and denote the set of points on the grid by Γ;
2: Based on the PGV data on $\mathbb{M}$, calculate the repair rate $g(i,j)$ for each grid point $(i,j) \in \Gamma$;
3: For each grid point $(i,j) \in \Gamma$, let $f(i,j) = c \cdot h(i,j) + g(i,j)$;
4: Create edges, faces and obtain a complete triangulation of surface $\mathbb{M}$ based on Γ;
5: Denote the approximate value of ϕ by $\bar{\phi}$ satisfying $\bar{\phi}(i,j) \simeq \phi(i\Delta_x + x_B, j\Delta_y + y_B)$. Let $\bar{\phi}(0,0) = 0$ and set the starting point B to *Near*. Define the neighbors of a grid element (i,j) to be the set $\Gamma_{(i,j)}$.
6: **while** *Near* list is not empty **do**
7:     Find a point (i,j) with the minimum value $\bar{\phi}$ in *Near* list, and set it to be *Frozen*.
8:     For each point $(i',j') \in \Gamma_{(i,j)}$, if (i',j') is not *Frozen*, for each face $\sigma \in \Sigma$, $\Sigma = \{\sigma, (i',j') \in \sigma\}$, calculate $\bar{\phi}(i',j')$ and update its value with the minimum one using (9) or (10).
9:     If (i',j') is *Far*, update its value by $\bar{\phi}(i',j')$ and add it in the *Near* list; otherwise update its value by minimum of $\bar{\phi}(i',j')$ and its current value.
10: **end while**
11: For each point $(i,j) \in \Gamma$, compute the gradient $G_0(i,j) = \nabla\bar{\phi}(i,j)$ using centered differences and normalize to obtain $G(i,j) = G_0(i,j)/||G_0(i,j)||$. Let $\gamma_0 = X_A$.
12: **while** $||\gamma_k - X_B||^2 > \varepsilon$ **do**
13:     Compute $\gamma_{k+1} = \gamma_k - \tau G(\gamma_k)$ using a numerical method (e.g. euler), where $\gamma_k \in \mathbb{R}^2$ is an approximation of $\gamma(t)$ at time $t = k\tau$.
14: **end while**
15: **return** γ.

Fig. 3. Framework of our approach.

A. Application of the algorithm to a 2D landform

We generate PGV data based on PSHA for a simple example in which the path of the link is planned on a planar (2D) region. A single line source (e.g. a fault line where earthquake epicenter may occur) of earthquakes of length 20 km located in a 2D landform region $[0, 100 \text{ km}] \times [0, 100 \text{ km}]$ is shown in Fig. 4(a). The coordinates of the two end points (x_A, y_A) and (x_B, y_B) of the line source are $(50 \text{ km}, 40 \text{ km})$ and $(50 \text{ km}, 60 \text{ km})$, respectively. Following the *bounded Gutenberg-Richter model* (Baker, 2008), this source produces earthquakes of magnitude between $m_{\min} = 5$ and $m_{\max} = 6.5$ with the probability density function (PDF)

$$f_M(m) = \frac{b \cdot 2.3026 \cdot 10^{-b(m-m_{\min})}}{1 - 10^{-b(m_{\max}-m_{\min})}}, \quad m \in [m_{\min}, m_{\max}].$$

We assume $b = 1$. We also assume that the spatial distribution of the epicenter of earthquakes is uniform along the line source. Usi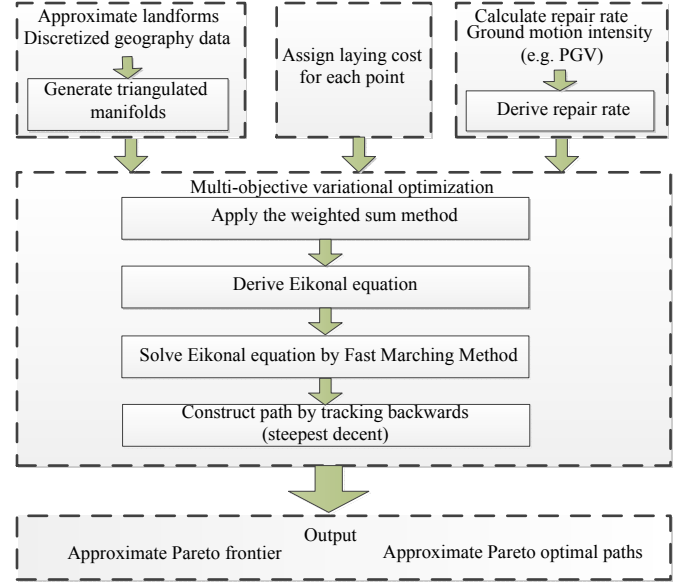ng the geometry of the source, the cumulative distribution function (CDF) of the epicenter distance r from a site (x,y) to the source is

$$F_R(R \le r) = \begin{cases} y_1, & y < y_A, d_A \le r \le d_B \\ y_2, & y_A \le y \le y_B, |x - x_A| \le r \le d_{\max} \\ y_3, & y > y_B, d_B \le r \le d_A, \end{cases}$$

where $y_1 = \frac{r_A - (y_A - y)}{y_B - y_A}$, $y_2 = \frac{\min(y_B, y+r_B) - \max(y_A, y-r_A)}{y_B - y_A}$, $y_3 = \frac{r_B - (y - y_B)}{y_B - y_A}$, $d_A = \sqrt{(x - x_A)^2 + (y - y_A)^2}$, $d_B = \sqrt{(x - x_B)^2 + (y - y_B)^2}$, $r_A = \sqrt{r^2 - (x - x_A)^2}$, $r_B = \sqrt{r^2 - (x - x_B)^2}$ and $d_{\max} = \max(d_A, d_B)$. The PDF $f_R(r)$ for r is obtained by taking the derivative of the above CDF.

Given potential earthquake magnitudes and locations, ground motion measures, such as PGV, have been observed to be well-represented by a log-normal distribution, i.e., $\ln v \sim \mathcal{N}(\mu(m,r), \sigma)$, where $\mu(m,r)$ and σ are the mean and standard deviation of v given by the attenuation relationship (Baker, 2008). In this case, we use the following predictive model for the mean of logarithmic PGV (in units of cm/s) (Cornell et al., 1979)

$$\mu(m,r) = 2.11 + 1.07m - 1.55\ln(r + 25),$$

and let $\sigma = 0.64$. By Law of Total Probability, the PDF of PGV for a site (x,y) is

$$p(v_{x,y}) = \int_M \int_R p(v_{x,y}|m,r) f_M(m) f_R(r) dm dr,$$

and then the mean PGV is $\bar{v}_{x,y} = \int_0^{+\infty} v_{x,y} p(v_{x,y}) dv$. Since there is no analytical expression for $\bar{v}_{x,y}$, we numerically compute the PDF of the PGV. In this computation, we quantize the PGV, magnitude and distance into equal bins with sizes 0.1 cm/s, 0.1 and 0.1 km, respectively.

The shaded surface map of the mean PGV derived based on above procedure is shown in Fig. 4(a). Then the PGV is

converted to repair rate by the following equation from Jeon and O'Rourke (2005).

$$\ln g(x, y) = 1.30 \cdot \ln \overline{v}_{x,y} - 7.21. \qquad (11)$$

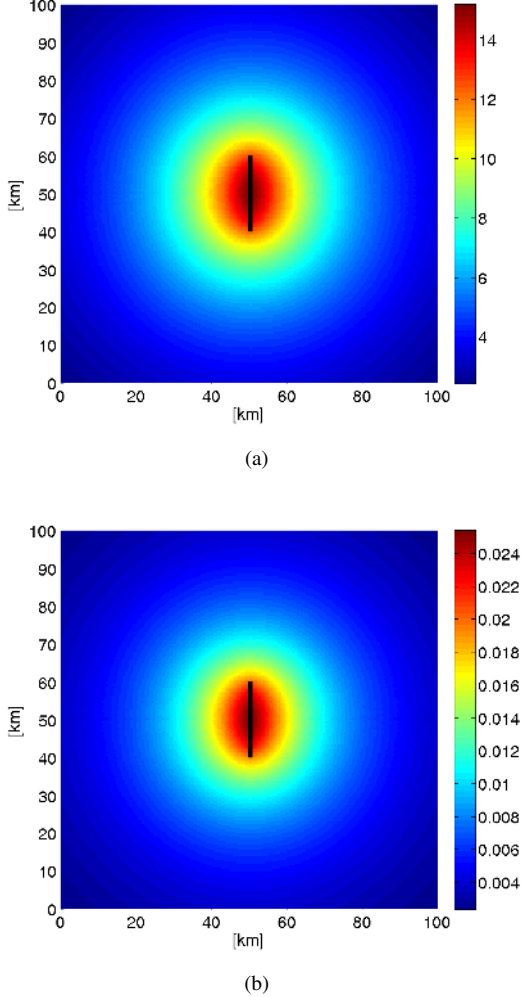The resulted repair rate is presented in Fig. 4(b).

(a)

(b)

Fig. 4. (a) Illustration of an example line source with length 20 km and the shaded surface map of mean Peak Ground Velocity. (b) The shaded surface map of repair rate.

We plan a path of the link from the site $(10\,\text{km}, 50\,\text{km})$ to the site $(90\,\text{km}, 50\,\text{km})$. In order to see how the laying cost of the link affects the results of the path planning, we set the weight of the length to different values, and then calculate the length and the total number of repairs of the resulting optimal links obtained by the method given in Section V. The results are shown in Table I and the corresponding paths are shown as in Fig. 5(a). From Table I and Fig. 5(a), we can observe the trade-off between the total number of repairs and the length of the link. Reducing the total number of repairs requires a longer link.

In order to derive the set of non-dominated optimal solutions for the two objectives: link length and total number of repairs, we vary the weight of the length (c) in the range from 10^{-4} to 10^{-1}, and then calculate the optimal paths increasing c by

ϵ in each path planning optimization. One can refer to Das and Dennis (1997) on how to produce a uniform distribution of points from all parts of the Pareto set. Fig. 5(b) shows the results. This non-dominated optimal solutions provide us with the results of the optimization problems of minimizing link laying cost (assuming link length reflects costs) subject to a constraint on the total number of repairs (or equivalently, on the level of survivalbility) and minimizing the total number of repairs (or maximizing survivalbility) subject to a constraint on the link laying cost (again, assuming link length reflects costs).
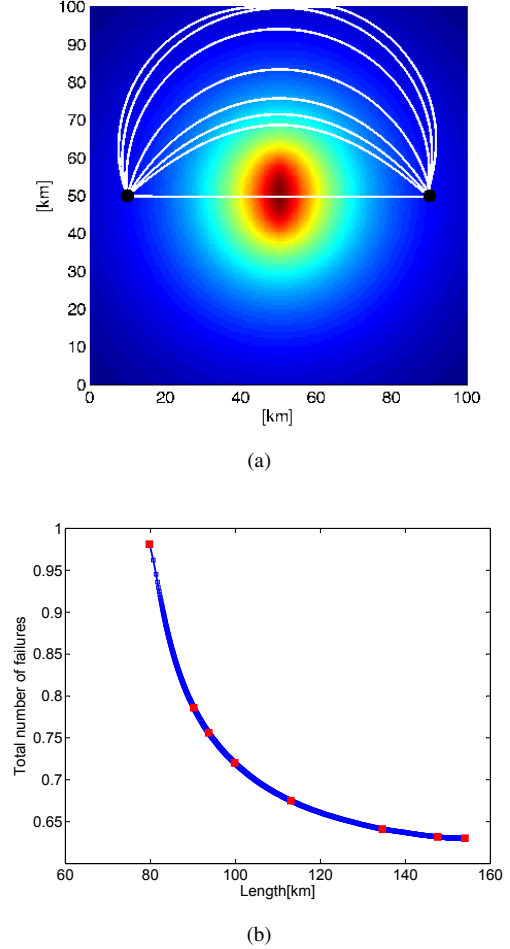

(a)

(b)

Fig. 5. (a) Optimal paths when $c = 10^{-4}$, 5×10^{-4}, 10^{-3}, 2.5×10^{-3}, 5×10^{-3}, 7.5×10^{-3}, 10^{-2}, 2.5×10^{-2}. (b) Non-dominated optimal solutions for the two objectives: (1) link Length, and (2) total number of repairs. The red squares are the non-dominated optimal values of the paths in (a).

B. Application of the algorithm to 3D landforms based on USGS seismic hazard map

In the next example, we use the earthquake hazard assessment data (PGA) from USGS (http://www.usgs.gov/) that is widely applied in seismic provisions of building codes, insurance rate structure, risk assessment, and other public policy.

TABLE I
DIFFERENT OPTIMAL PATHS TAKING INTO ACCOUNT THE LAYING COST AND THE TOTAL NUMBERS OF REPAIRS IN THE CASE OF THE EXAMPLE LINE
SOURCE.

c $(\times 10^{-3})$	0.1	0.5	1	2.5	5	7.5	10	25
Length (km)	154.03	147.63	134.68	113.05	99.80	93.70	90.15	80.00
Total number of repairs	0.630	0.632	0.641	0.675	0.720	0.756	0.787	0.981

It contains space-delimited, rectangularly gridded data in 0.05 degree increments in longitude and latitude. We plan paths of links in two different regions $\mathbb{D}_1$ $\left((40.23°, -124.30°) \sim (32.60°, -114.30°)\right)$ and $\mathbb{D}_2$ $\left((40.54°, -95.00°) \sim (32.75°, -85.50°)\right)$, as shown in Fig. 6.

The land of region $\mathbb{D}_1$, including almost the whole California state and a large part of Nevada, locates on the west coast of US closed to the Pacific Ocean. There are several fault lines throughout $\mathbb{D}_1$, of which the famed San Andreas fault line is a major one. The northeastern land of region $\mathbb{D}_1$ is a large range of desert and the wide and generally flat land of southeastern $\mathbb{D}_1$ is punctuated by some irregular mountain peaks such as the Mt Whitney at 14,494 ft. The famous Central Valley, which is closed to the San Andreas fault line, locates in the center of $\mathbb{D}_1$.

Region $\mathbb{D}_2$ is in the US central and consists of several states such as Missouri, Illinois, Indiana, Kentucky, Tennessee, Alabama, Mississippi and Arkansas. The most of part of region $\mathbb{D}_2$ is plain, especially in the central, a basin landform locates on the common border of Missouri, Arkansas, Mississippi and Tennessee. Although no such long fault line like the San Andreas fault line passes through region $\mathbb{D}_2$, there is still a high possibility of a big earthquake to occur in the basin land.
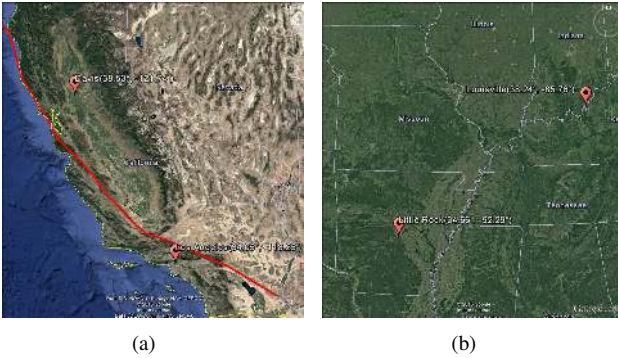

(a)

(b)

Fig. 7.   The shaded surface maps of the PGV (cm/s): (a) Region $\mathbb{D}_1$, (b) Region $\mathbb{D}_2$. Data is provided by USGS.

(a)   (b)

Fig. 6.   Geography: (a) Region $\mathbb{D}_1$, (b) Region $\mathbb{D}_2$. Source: Google Earth.

To calculate the repair rate of the link, we first obtain the PGA (2% probability of exceedance in 50 years, Vs30 = 760 m/s) for each gridded geographical point and then convert it to PGV by the following equation from Wald (1999),

$$\log_{10}(v) = 1.0548 \cdot \log_{10}(\text{PGA}) - 1.1556. \quad (12)$$

The shaded surface map of PGV of the two regions are shown in Fig. 7. Then the PGV is converted to repair rate by (11).
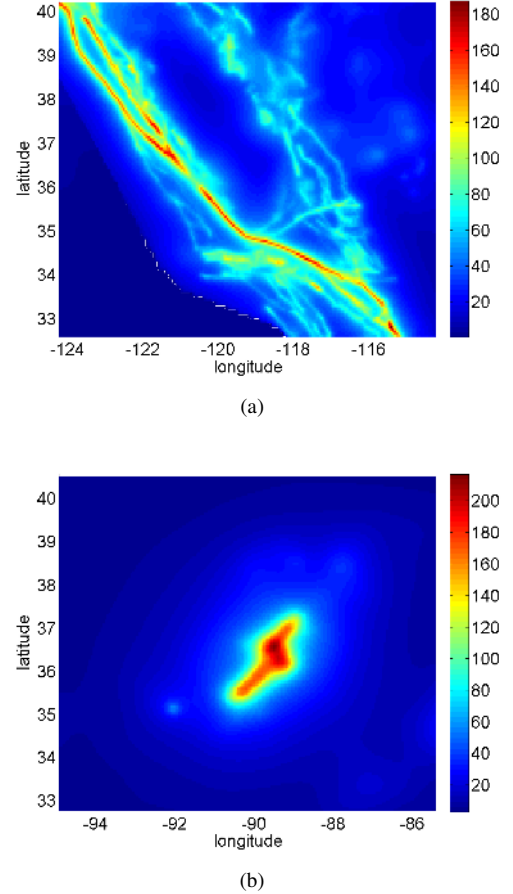
To calculate geodesic distance, we downloaded the elevation data for the corresponding areas from the National Oceanic and Atmospheric Administration (http://maps.ngdc.noaa.gov). It contains space-delimited, rectangularly gridded data with the same resolution as the repair rate data in latitude and longitude. The resolution of elevation is 30 m $\sim$ 90 m. Coordinate transformation is applied for both the repair rate data set and the geographic data to convert them from latitude and longitude coordinates to Universal Transverse Mercator coordinates. Using the landforms model described in Section IV, $60,800$ faces are created for region $\mathbb{D}_1$ and $58,900$ faces are created for region $\mathbb{D}_2$, and the triangulated manifold approximation of the landforms are shown in Fig. 8 and Fig. 10.

In region $\mathbb{D}_1$, we aim to plan the path of a link from Los Angles $(34.05°, -118.25°)$ to Davis $(38.53°, -121.74°)$. From Fig. 6(a) and Fig. 7(a), we can see that the link connecting

the two cities should pass through the San Andreas fault line unavoidably and that it extends more than 1000 km through California. By letting $g(S) = 0$ and $h(S) = 0$ in Problem 2, we can calculate the length of the shortest path without considering repairs and the length of the path with minimum total number of repairs, which are 598.03 km and 637.47 km, respectively. Fig. 8 shows the optimal paths when the weights of the length of the link are equal to 0.0252, 0.2188, 0.3802 and 10. From Fig. 8, we can see that to reduce the total number of repairs through minimizing the number of points on the link that may be affected by an earthquake, the angle between the optimal link and the San Andreas fault line increases gradually around Los Angles. It then moves away from the San Andreas fault line until it approximates the one with the minimum total number of repairs. As in the previous example, we set the

link from Little Rock $(34.66°, −92.29°)$ to Louisville $(38.24°, −85.76°)$ in region $\mathbb{D}_2$. In comparison with region $\mathbb{D}_1$, there is no such long fault line as the San Andreas fault line in region $\mathbb{D}_2$. A link connecting the two cities can avoid the hazard zone if it is long enough. To calculate the non-dominated optimal solutions, we set the weight of the length to be in the range between 10^{-4} and 10 again. Fig. 11 presents the results. The length of the shortest path without considering repairs and the length of the path with minimum total number of repairs are 6.962×10^2 km and 1.628×10^3 km, respectively. Fig. 10 shows the optimal paths when the weights of the length of the link are equal to 3.8905×10^{-4}, 6.6×10^{-3}, 6.8×10^{-3}, 0.1514 and 10. As in the first example, to reduce the total number of repairs, the link will be very far away from the fault line in which case the length of the link will increase significantly. From Fig. 11, we can see that increasing the length of the link from 700 km to 800 km can reduce the total number of repairs significantly (around 100 repairs). However, increasing the length of the link from 1000 km to 1600 km will lead to very limited reduction in the number of repairs. This provides valuable insight to design tradeoffs between laying cost-effectiveness and survivability.
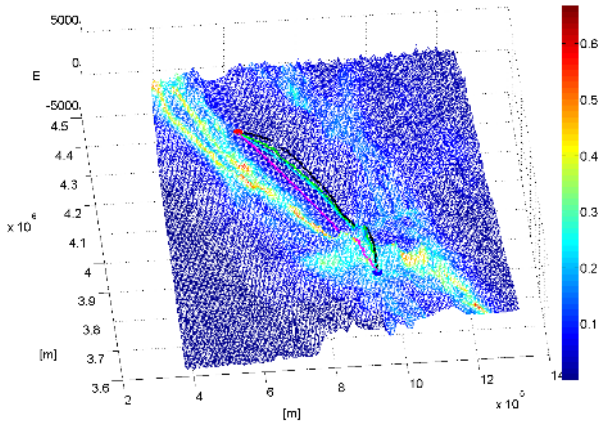

Fig. 8. (a) Illustration of triangulation in the UTM coordinate system, repair rate and paths when $c = 0.0252$ (black), 0.2188 (green), 0.3802 (cyan) and $c = 10$ (magenta). The color represents repair rate.

weight of the length to be from 10^{-3} to 10, and then calculate the set of non-dominated optimal solutions. Fig. 9 shows the results.
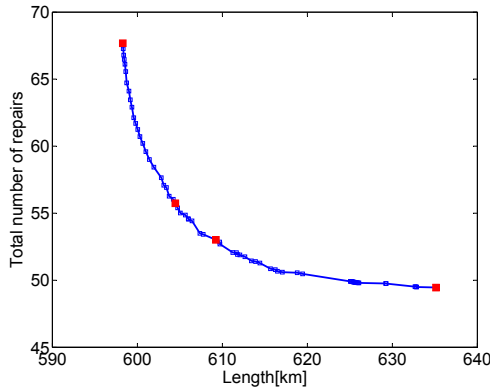

Fig. 9. Non-dominated optimal solutions for the two objectives: (1) link Length, and (2) total number of repairs. The red squares are the non-dominated optimal values of the paths in Fig. 8.

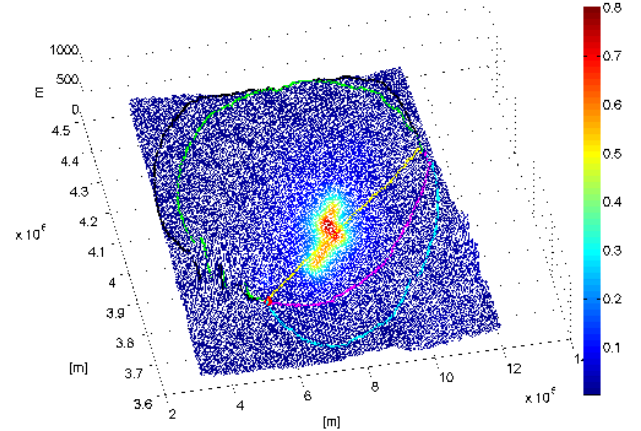In the next and final example, we aim to plan the path of a

Fig. 10. (a) Illustration of triangulation in the UTM coordinate system, repair rate and paths when $c = 3.8905 \times 10^{-4}$ (black), 6.6×10^{-3} (green), 6.8×10^{-3} (cyan), 0.1514 (magenta) and $c = 10$ (yellow). The color represents repair rate.

VII. CONCLUSION

We have considered the problem of how to lay a critical infrastructure link to connect two points across an earthquake prone area. We have formulated the problem as a multi-objective variational optimization that considers link laying cost and total number of repairs as the two objectives. The Earth surface has been modeled as a triangulated manifold, and we have introduced ground motion intensity measures of earthquake events to calculate the total number of repairs. Using the weighted sum method, the multi-objective variational optimization problem has been transformed into a single objective variational problem, which can be described in terms of Eikonal equation and solved by the computationally
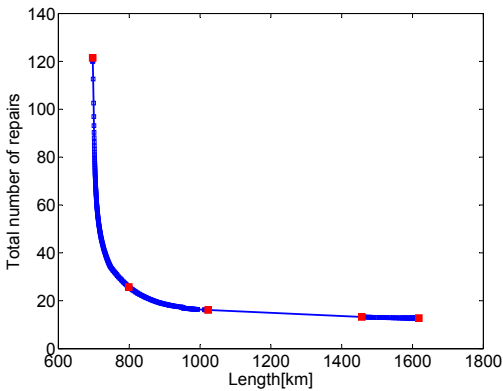
Fig. 11. Non-dominated optimal solutions for the two objectives: (1) link Length, and (2) total number of repairs. The red squares are the non-dominated optimal values of the paths in Fig. 10.

light FMM. Through many numerical FMM simulations, we have obtained the non-dominated optimal solutions for the two objectives, which enable us to solve two single objective optimization problems of minimizing the laying cost subject to a constraint on the total number of repairs, and minimizing the total number of repairs subject to a constraint on the laying cost. Although our approach focus one link, it provides a step-tool for optimizing more complex critical infrastructure link topologies.

REFERENCES

Adachi, T. and Ellingwood, B. R. (2009). Serviceability assessment of a municipal water system under spatially correlated seismic intensities. *Computer-Aided Civil and Infrastructure Engineering*, 24(4):237–248.

Alliance, A. L. (2001). Seismic fragility formulations for water systems, Part I-Guideline. http://www.americanlifelinesalliance.com/pdf/Part_1_Guideline.pdf.

Baker, J. (2008). An introduction to probabilistic seismic hazard analysis (PSHA). white paper. version 1.3. Stanford University. https://web.stanford.edu/~bakerjw/Publications/Baker_(2008)_Intro_to_PSHA_v1_3.pdf.

Balogun, A., Matori, A., Lawal, D. U., and Chandio, I. (2012). Optimal oil pipeline route selection using GIS: Community participation in weight derivation and disaster mitigation. In *proc International Conference on Future Environment and Energy 2012*, volume 28, pages 100–104.

Bector, C. and Husain, I. (1992). Duality for multiobjective variational problems. *Journal of Mathematical Analysis and Applications*, 166(1):214–229.

Bruneau, M., Chang, S. E., Eguchi, R. T., Lee, G. C., O'Rourke, T. D., Reinhorn, A. M., Shinozuka, M., Tierney, K., Wallace, W. A., and von Winterfeldt, D. (2003). A framework to quantitatively assess and enhance the seismic resilience of communities. *Earthquake spectra*, 19(4):733–752.

Burago, D., Burago, Y., and Ivanov, S. (2001). *A course in metric geometry*, volume 33. American Mathematical Society Providence.

Cao, C. (2015). *Cost effective and survivable cabling design under major disasters*. PhD thesis, City University of Hong Kong.

Cao, C., Wang, Z., Zukerman, M., Manton, J., Bensoussan, A., and Wang, Y. (2016). Optimal cable laying across an earthquake fault line considering elliptical failures. *to appear in IEEE Transactions on Reliability*.

Cao, C., Zukerman, M., Wu, W., Manton, J. H., and Moran, B. (2013). Survivable topology design of submarine networks. *Journal of Lightware Technology*, 31(5):715–730.

Carter, L., Burnett, D., Drew, S., Marle, G., Hagadorn, L., Bartlett-McNeil, D., and Irvine, N. (2009). *Submarine cables and the oceans: connecting the world*. UNEP-WCMC Biodiversity Series No.31. ICPC/UNEP/UNEP-WCMC.

Carter, L., Gavey, R., Talling, P., and Liu, J. (2014). Insights into submarine geohazards from breaks in subsea telecommunication cables. *Oceanography*, 27(2):58–67.

Cavalieri, F., Franchin, P., Buriticá Cortés, J. A., and Tesfamariam, S. (2014). Models for seismic vulnerability analysis of power networks: comparative assessment. *Computer-Aided Civil and Infrastructure Engineering*, 29(8):590–607.

Chang, K. (2013). *Introduction to Geographic Information Systems*. McGraw-Hill, New York, 7th edition.

Chen, W. W., Shih, B.-J., Chen, Y.-C., Hung, J.-H., and Hwang, H. H. (2002). Seismic response of natural gas and water pipelines in the Ji-Ji earthquake. *Soil Dynamics and Earthquake Engineering*, 22(9):1209–1214.

Cimellaro, G. P., Villa, O., and Bruneau, M. (2014). Resilience-based design of natural gas distribution networks. *Journal of Infrastructure Systems*, 21(1):05014005–1–05014005–14.

Cobanli, O. (2014). Central Asian gas in Eurasian power game. *Energy Policy*, 68:348–370.

Cornell, C., Banon, H., and Shakal, A. (1979). Seismic motion and response prediction alternatives. *Earthquake Engineering & Structural Dynamics*, 7(4):295–315.

Das, I. and Dennis, J. E. (1997). A closer look at drawbacks of minimizing weighted sums of objectives for Pareto set gen-

eration in multicriteria optimization problems. *Structural optimization*, 14(1):63–69.

Dey, P. and Ogunlana, S. O. (1999). Decision support system for pipeline route selection. *Cost Engineering*, 41(10):29–35.

Dübendorfer, T. P. (2005). *Impact analysis, early detection and mitigation of large-scale Internet attacks*. PhD thesis, Swiss Federal Institute of Technology Zürich.

Eriksson, K., Estep, D., and Johnson, C. (2013). *Applied Mathematics: Body and Soul: Volume 1: Derivatives and Geometry in IR3*. Springer Science & Business Media.

Esposito, S. (2011). *Seismic risk analysis of gas distribution networks*. PhD thesis, University of Naples Fegerico II.

Esposito, S., Iervolino, I., d'Onofrio, A., Santo, A., Cavalieri, F., and Franchin, P. (2015). Simulation-based seismic risk assessment of gas distribution networks. *Computer-Aided Civil and Infrastructure Engineering*, 30(7):508–523.

Florinsky, I. V. (2012). *Digital terrain analysis in soil science and geology*. Academic Press.

Fragiadakis, M. and Christodoulou, S. E. (2014). Seismic reliability assessment of urban water networks. *Earthquake Engineering & Structural Dynamics*, 43(3):357–374.

Greenspan, D. (2000). *Introduction to partial differential equations*. Dover Publications, INC., Mineola, New York.

Hwang, H., Chiu, Y.-H., Chen, W.-Y., and Shih, B.-J. (2004). Analysis of damage to steel gas pipelines caused by ground shaking effects during the Chi-Chi, Taiwan, earthquake. *Earthquake spectra*, 20(4):1095–1110.

Jeon, S.-S. and O'Rourke, T. D. (2005). Northridge earthquake effects on pipelines and residential buildings. *Bulletin of the Seismological Society of America*, 95(1):294–318.

Kimmel, R. and Sethian, J. (1998). Computing geodesic paths on manifolds. *Proceedings of the National Academy of Sciences*, 95(15):8431–8435.

Kimmel, R. and Sethian, J. (2001). Optimal algorithm for shape from shading and path planning. *Journal of Mathematical Imaging and Vision*, 14(3):237–244.

Kobayashi, M. (2014). Experience of infrastructure damage caused by the great east Japan earthquake and countermeasures against future disasters. *IEEE Communications Magazine*, 52(3):23–29.

Lanzano, G., Salzano, E., de Magistris, F. S., and Fabbrocino, G. (2013). Seismic vulnerability of natural gas pipelines. *Reliability Engineering & System Safety*, 117:73–80.

LaPerrière, S. (2007). Taiwan earthquake fiber cuts: a service provider view. https://www.nanog.org/meetings/nanog39/presentations/laperriere.pdf.

Lee, J. (1991). Comparison of existing methods for building triangular irregular network, models of terrain from grid dig-

ital elevation models. *International Journal of Geographical Information System*, 5(3):267–285.

Liu, A. (2009). Response analysis of a submarine cable under fault movement. *Earthquake Engineering and Engineering Vibration*, 8(1):159–164.

Macharia, P. M. (2014). GIS analysis and spatial modelling for optimal oil pipeline route location. a case study of proposed Isiolo Nakuru pipeline route. In *Proceedings of Sustainable Research and Innovation Conference*, pages 91–94.

Martínez, D., Velho, L., and Carvalho, P. C. (2005). Computing geodesics on triangular meshes. *Computers & Graphics*, 29(5):667–675.

mi2g (2005). More than 1% GDP drop estimated per week of Internet blackout. www.mi2g.com/cgi/mi2g/press/220705.php.

Miettinen, K. (1999). *Nonlinear Multiobjective Optimization*. Kluwer Academic Publishers, Boston.

Neumayer, S., Zussman, G., Cohen, R., and Modiano, E. (2011). Assessing the vulnerability of the fiber infrastructure to disasters. *IEEE/ACM Transactions on Networking*, 19(6):1610–1623.

O'Rourke, T. D., Toprak, S., and Sano, Y. (1998). Factors affecting water supply damage caused by the Northridge earthquake. In *Proceedings of the 6th US National Conference on Earthquake Engineering*, pages 1–12, Seattle, WA, USA.

Peucker, T. K., Fowler, R. J., Little, J. J., and Mark, D. M. (1978). The triangulated irregular network. In *Amer. Soc. Photogrammetry Proc. Digital Terrain Models Symposium*, pages 516–540.

Pineda-Porras, O. and Najafi, M. (2010). Seismic damage estimation for buried pipelines: Challenges after three decades of progress. *Journal of Pipeline Systems Engineering and Practice*, 1(1):19–24.

Qiu, W. (2011). Submarine cables cut after Taiwan earthquake in Dec 2006. http://submarinenetworks.com/news/cables-cut-after-taiwan-earthquake-2006.

Røstum, J. (2000). *Statistical modelling of pipe failures in water networks*. PhD thesis, Norwegian University of Science and Technology.

Saraf, S. (2009). Acute and nonobtuse triangulations of polyhedral surfaces. *European Journal of Combinatorics*, 30(4):833–840.

Schuster, R. L., editor (1991). *March 5, 1987, Ecuador Earthquakes: Mass Wasting and Socioeconomic Effects*. National Academies Press, Washington, D.C.

Sethian, J. (1996). A fast marching level set method for monotonically advancing fronts. *Proceedings of the National Academy of Sciences*, 93(4):1591–1595.

Sethian, J. (1999a). Fast marching methods. *SIAM Review*, 41(2):199–235.

Sethian, J. (1999b). *Level Set Methods and Fast Marching Methods: Evolving Interfaces in Computational Geometry, Fluid Mechanics, Computer Vision, and Materials Science*. Cambridge Press, New York, second edition.

Toprak, S. (1998). *Earthquake effects on buried lifeline systems*. PhD thesis, Cornell University.

Toprak, S. and Taskin, F. (2007). Estimation of earthquake damage to buried pipelines caused by ground shaking. *Natural hazards*, 40(1):1–24.

Villaverde, R. (2009). *Fundamental Concepts of Earthquake Engineering*. CRC Press, Boca Raton.

Wald, D. J. (1999). Relationships between peak ground acceleration, peak ground velocity, and modified Mercalli intensity in California. *Earthquake Spectra*, 15(3):557–564.

Wang, Y. and Au, S.-K. (2009). Spatial distribution of water supply reliability and critical links of water supply to crucial water consumers under an earthquake. *Reliability Engineering & System Safety*, 94(2):534–541.

Wang, Y. and O'Rourke, T. D. (2008). *Seismic performance evaluation of water supply systems*. Multidisciplinary Center for Earthquake Engineering Research, Buffalo, NY.

Xin, S.-Q. and Wang, G.-J. (2007). Efficiently determining a locally exact shortest path on polyhedral surfaces. *Computer-Aided Design*, 39(12):1081–1090.

Yildirim, Y., Aydinoglu, A. C., and Yomralioglu, T. (2007). GIS based pipeline route selection by ArcGIS in Turkey. In *Proceedings of the 27th Annual ESRI User Conference*.

Yung, E. (2011). Project profile for South-East Asia Japan Cable System (SJC) Hong Kong segment. Technical Report 4575-OR002, Atkins China Ltd. http://www.epd.gov.hk/eia/register/profile/latest/dir213/dir213.pdf.

Zhao, M., Chow, T.W.S., Tang, P., Wang, Z., Guo, J., and Zukerman, M. (2016). Route selection for cabling considering cost minimization and earthquake survivability via a semi-supervised probabilistic model. *to appear in IEEE Transactions on Industrial Informatics*.

Zohra, H. F., Mahmouda, B., and Luc, D. (2012). Vulnerability assessment of water supply network. *Energy Procedia*, 18:772–783.